

Characterization of $\text{ZnGa}_2\text{O}_4:\text{Cr}^{3+}$ doped with antisite defects

A dissertation for

Course code and Course Title: PHY-651 Dissertation

credits: 16

submitted in partial fulfillment of Master degree

M.sc in physics (solid state physics)

by

DIVYA VAGHEKAR

22PO430008

ABC ID :- 649-274-972-140

PRNO :- 201905628

under the supervisor of

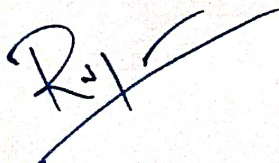
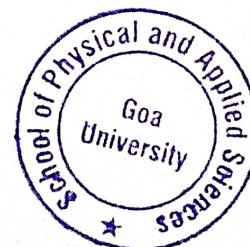
DR. KAUSTUBH R.S. PRIOLKAR

school of physical and applied science
physics discipline



GOA UNIVERSITY
MAY 2024

Examined by:


A handwritten signature in blue ink, appearing to be 'R. S. Priolkar'.

Seal of the School

DECLARATION BY STUDENT

I hereby declare that the data presented in this Dissertation report entitled, "Characterization of Zinc gallate while chromium doped with antisite defects" is based on the results of investigations carried out by me in the Physics at the School of Physical and Applied Sciences, Goa University under the Supervision of Dr.Kaustubh R.S.Priolkar and the same has not been submitted elsewhere for the award of a degree or diploma by me. Further, I understand that Goa University or its authorities will be not be responsible for the correctness of observations / experimental or other findings given the dissertation.

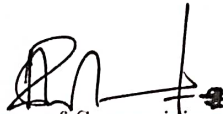
I hereby authorize the University authorities to upload this dissertation on the dissertation repository or anywhere else as the UGC regulations demand and make it available to any one as needed.

 Divya Vaghekar)
Signature and Name of Student
Seat no.:- 22P0430008

Date: 8/5/24
Place: Goa University

COMPLETION CERTIFICATE

This is to certify that the dissertation report "Characterization of Zinc Gallate while chromium doped with antisite defects" is a bonafide work carried out by Miss Divya Vaghekar under my supervision in partial fulfilment of the requirements for the award of the degree of (M.Sc in Physics) in the physics at the School of physical and applied sciences,Goa university.


Signature and Name of Supervising Teacher

Kaustubh R. S. Priolkar

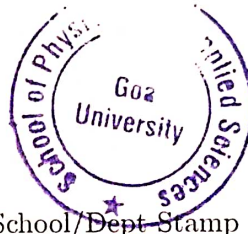
Date:- 8/5/24



Signature of Dean of the School/HoD of Dept

Date:-

Place:Goa University



School/Dept Stamp

Contents

1	Introduction	ix
1.1	Persistent luminescence	ix
1.2	Persistent luminescence background	x
1.3	Long Lasting Phosphorescence mechanisms	xi
1.3.1	Aitasalo model	xi
1.3.2	Matsuzava model	xi
1.3.3	Dorenbos model	xii
1.3.4	Clabau model	xii
1.4	Applications of LLP materials	xiii
1.5	Materials of LLP	xiv
1.6	Objectives	xv
2	Experimental techniques	xvi
2.1	Introduction	xvi
2.1.1	Sample preparation method	xvi
2.1.2	X-ray diffraction	xvii
2.2	UV-Visible absorption spectroscopy	xviii
2.3	Photoluminescence spectroscopy	xix
2.3.1	PL excitation	xx
2.3.2	PL emission	xxi
2.4	Long Lasting Phosphorescence	xxii
2.5	Raman Spectroscopy	xxii
3	Results of ZGGO	xxiv
3.1	XRD patterns	xxiv
3.2	UV-vis absorption spectroscopy	xxv
3.3	Photoluminescence Spectroscopy	xxvi
3.3.1	PL excitation	xxvi
3.3.2	PL emission	xxvii
3.4	Long Lasting Phosphorescence decay	xxviii
3.4.1	LLP 360ex OnOff for ZGGO	xxix
3.5	Raman spectroscopy	xxx
3.6	Anomalous XRD spectroscopy	xxx
3.7	References	xxxiv

List of Figures

1.1	Bologna rocks	x
1.2	LLP mechanism by Aitasalo	xi
1.3	LLP mechanism by Matsuzawa	xii
1.4	LLP mechanism by Dorenbos	xii
1.5	LLP mechanism of Clabau model	xiii
1.6	Examples of LLP	xiv
2.1	$\text{ZnGa}_2\text{Cr}_{0.01}\text{O}_4$ sample	xvii
2.2	X-ray Diffraction instrument	xviii
2.3	XRD graphs of $\text{ZnGa}_2\text{Cr}_{0.01}\text{O}_4$ sample	xviii
2.4	UV-Visible reflectance spectra of ZGO sample	xix
2.5	UV-Visible instrument	xix
2.6	PL instrument image	xx
2.7	PL exc697 of ZGO sample	xxi
2.8	PL em200 of ZGO sample	xxi
2.9	Raman spectroscopy instrument	xxii
2.10	Raman spectroscopy of $\text{ZnGa}_2\text{Cr}_{0.01}\text{O}_4$ (fit.gaussianA1g)	xxiii
2.11	Raman spectroscopy of $\text{ZnGa}_2\text{Cr}_{0.01}\text{O}_4$ (fit.gaussianT2g)	xxiii
3.1	XRD graphs of ZGGO samples	xxiv
3.2	UV-visible reflectance spectra of all ZGGO samples	xxv
3.3	PL excitation695 of ZGGO (0%)	xxvi
3.4	PL excitation695 of ZGGO (0.05%)	xxvi
3.5	PL excitation of ZGGO (0.10%)	xxvi
3.6	PL excitation of ZGGO (0.20%)	xxvi
3.7	PL excitation of ZGGO (0.40%)	xxvii
3.8	PL emission of 360 ZGGO all samples	xxvii
3.9	d^3 Tanabe sugano diagram for Cr^{3+} in octahedral ZGGO	xxviii
3.10	LLP decay curve of all ZGGO samples	xxviii
3.11	LLP 360ex OnOff for ZGGO (0%)	xxix
3.12	LLP 360ex OnOff for ZGGO (0.05%)	xxix
3.13	LLP 360ex OnOff for ZGGO (0.10%)	xxix
3.14	LLP 360ex OnOff for ZGGO (0.20%)	xxix
3.15	LLP 360ex OnOff for ZGGO (0.40%)	xxix
3.16	Raman spectra of all ZGGO samples (fit.gaussian) A1g mode . .	xxx

3.17 Raman spectra of all ZGGO samples (fit.gaussian T2g)	xxxix
3.18 Raman spectra of all ZGGO samples (fit.gaussian T1g)	xxxix
3.19 Graphs of ZGG01,ZGGO,ZGGO2,ZGGO4 at different energies	xxxix
3.20 Area of 222 peak at different incident energies.	xxxix
3.21 Area of 422 peak at different incident energies.	xxxix

Acknowledgement

I would to express my deepest gratitude to the my project guide Dr.K.R.S.Priolkar for providing me with valuable advice, guidance and support throughout the entire project. I would also like to thank all of the participants who took part in these project, without whom this research would not have been possible. I would like to thank Dr. Ramesh pai , dean of school of physical and applied sciences for giving me an opportunity to carry out my dissertation work, my profound gratitude Dr.Venkatesh hathwar, programme director off physics discipline for providing the essential infrastructure facilities and permission to proceed with my dissertation work.

I would also like to thank my classmates who helped with data collection and analysis as well as my parents for providing the necessary materials. i extend to heartfelt gratitude to Goa university for providing necessary resources, facilities and academic environment conductives to scholarly inquiry greatly facilities the competition of the thesis.

Abstract

The interest in the family of ZnGa_2O_4 spinel compound doped with Cr^{3+} has been aroused in the most recent years. It is very bright persistent phosphor able to emit a near infrared light for hours following uv (band to band excitation) or visible Cr^{3+} excitation illumination. We show that the dopant concentration plays an important role in the total persistent luminescence of the material. Persistent luminescence increases as a consequence of antisite defects. We have analysed XRD, UV-Visible, photoluminescence excitation, emission and Raman and Anomalous XRD data on a series of ZnGa_2O_4 samples doped with Ge, $\text{Zn}_{1+x}\text{Ga}_{2-2x}\text{Ge}_x\text{O}_4:\text{Cr}^{3+}$, and attempted to provide an explanation to the observed persistent luminescence. Persistence luminescence initially increases with doped Ge due to increased antisite defects around Cr. At smaller dopant concentration, both Ge and Zn replace Ga^{3+} in octahedral sites. This increased Ge doping, Ge^{4+} replaces Zn^{2+} in the tetrahedral sites, increasing the number of Zn^{2+} ion at octahedral sites. This is detrimental to LLP and it decreases.

Chapter 1

Introduction

1.1 Persistent luminescence

Persistent luminescence it means material emits light in the visible range appreciably for hours even after the irradiation source has been off. The storage of the irradiation energy by traps is to be responsible for long decay time of persistence luminescence. It is the most rare earth application based on lattice defects. Long decay period in persistent phosphors can be attributed to traps with different trapping depth. The trapping depth can be defined as the energy is to be responsible to release the electrons from a trap.

Persistent luminescence is a luminescence phenomenon wherein the materials emit light usually in the visible range, from few minutes to several hours, even after their exposure to radiation (visible, UV or higher energy) is stopped. This phenomenon is also known as long lasting phosphorescence (LLP) or thermoluminescence or afterglow or sometimes phosphorescence. The term phosphorescence is often misleading in this context since the process does not involve the triplet to singlet transitions. The delay in emission in LLP materials is caused by the impurities present in the material.

It has aroused a great zeal and enthusiasm among the researchers worldwide owing to their promising potential applications and remarkable versatile functionality. A higher emission lifetime without an impulse of constant energy input allows several opportunities to a persistent luminescent materials not only in optoelectronics but also in fields as diverse as biomedical sciences and energy conserving devices. Persistent luminescence of materials, also known as long-lasting phosphorescence (LLP), is based on the transient storage of radiation in the form of traps holes and electrons, followed by the slow detrapping and radiative recombination of the carriers. This gives rise to a visible-light emission lasting for minutes or hours, suitable for many applications as night or dark environment vision displays (emergency signs, toys, etc.) When light emission occurred in the region of partial transparency of living tissues, that is, in the red to near-infrared, this long lasting phosphorescence nanoparticles can be used for

in vivo imaging of small animals as well as active targeting of various cancerous cells in vitro through specific ligand/receptor interaction. As a major asset of this process, the particles can be excited ex vivo before injection, which involves autofluorescence otherwise observed when living tissues are also excited.

1.2 Persistent luminescence background

The persistent luminescence phenomenon has been known to mankind for a thousand of years. Descriptions have been found in ancient Chinese paintings that remained visible during the night, by mixing the colors with a special kind of pearl shell. The first scientifically described observation of persistent luminescence dates back to 1603, where shoemaker and alchemist Vincenzo Casciarolo discovered the famous Bologna stone. The curious glow of this stone was described by Fortunius Licetus in the *Lithosphorus Sive De Lapide Bononiensi* in 1640, and was most probably caused by barium sulfide present in the rock. Natural impurity in the stone was responsible for long duration of the afterglow.



Figure 1.1: Bologna rocks

Until the end of 20th century, very little research was done on the phenomenon of persistent luminescence. Zinc sulfide (ZnS) doped with copper (and later co-doped with cobalt) was the most famous and widely used persistent phosphor. ZnS based phosphors, such as $\text{ZnS}:\text{Cu}^+$ were found to have persistent times as long as 40 minutes. The effects of co-doping were also investigated, for example, co-doping $\text{ZnS}:\text{Cu}^+$ with Co^{2+} doubled the persistent time of the phosphor. However, still the brightness and lifetime of the material were rather low for practical purposes. To resolve this problem, radioactive element traces of such as tritium were often introduced in the powders to stimulate the brightness and lifetimes of the light emission. But even then, a commercial glow in the dark object had to contain a luminescent material large amount of a yield an acceptable afterglow. The long persistent phosphors of next generation comprised the alkaline earth sulfides, such as CaS and SrS. These phosphors known as Lenard's phosphors.

When Wiedemann (1888) recognized luminescence as the antithesis to incandescence, he also classified luminescences into six kinds according to the method of

excitation. No better basis of classification is available today. He recognizes photoluminescence, thermoluminescence, electroluminescence, crystalloluminescence, triboluminescence and chemiluminescence. Photoluminescence of solid is excited by light itself and is subdivided by fluorescence and phosphorescence.

Thermoluminescence is light from gentle heating. Electroluminescence appears from gases in electrical fields. Crystalloluminescence and triboluminescence occur when solutions crystallize or when crystals are crushed or broken, and chemiluminescence may appear during chemical reaction.

1.3 Long Lasting Phosphorescence mechanisms

Different mechanisms have been proposed since then, detailing the nature and origin of the charge carriers and the traps. Some of the major mechanisms are given below.

1.3.1 Aitasalo model

Aitasalo mechanism proposed by, it was presumed that traps from direct excitation energy of transition. The energy trapped was then released during thermal process leading to electron-hole recombination at room temperature. Eu^{2+} ion rare earth element was utilized by this energy, causing the $4f \rightarrow 5d$ excitation evident in emission spectra of phosphor.

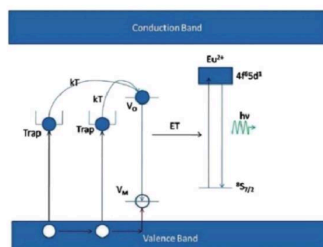


Figure 1.2: LLP mechanism by Aitasalo

1.3.2 Matsuzawa model

Matsuzawa reported the standard $\text{SrAl}_2\text{O}_4:\text{Eu}^{2+}$ phosphor a sensitizer Dysprosium with co doped that managed to hold visible brightness back throughout the entire night.

In this model, holes were considered to be the major charge carriers. When a photon is incident on the material, Eu^{2+} absorbs the energy and turns into Eu^{1+} ion with a hole escaping to the valence band. This hole is trapped by Dy^{3+} ion to become Dy^{4+} . When thermal energy is available of a sufficient amount, it

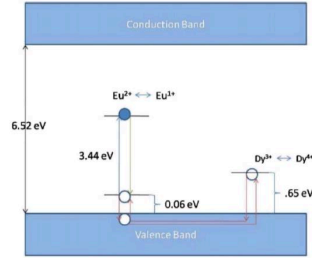


Fig. 10. The schematic of the energy levels in $\text{SrAl}_2\text{O}_4:\text{Eu}^{2+}, \text{Dy}^{3+}$ phosphor as generated by Matsuzawa.

Figure 1.3: LLP mechanism by Matsuzawa

detraps the hole which is released back to the valence band and then to the Eu^{1+} ion. Then, Eu^{1+} returns to its ground state Eu^{2+} with the emission of a photon.

1.3.3 Dorenbos model

In these model, electron is excited from 4f level of europium which lies close to valence band, to 5d level which is close to conduction band. This electron is released into the conduction band from where it is trapped by the rare earth trivalent co-dopant. Thermal energy detrapping electron to conduction band and it subsequently recombines with the hole left behind, resulting in emission.

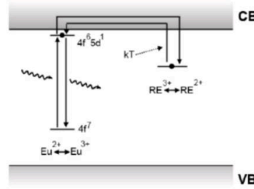


Figure 1.4: LLP mechanism by Dorenbos

1.3.4 Clabau model

This is an revised model of $\text{SrAl}_2\text{O}_4:\text{Eu}^{2+}, \text{Dy}^{3+}$. According to this model electron transport between traps and luminescent centres occurs through direct transfer and not through the conduction band. This required a close proximity between the luminescent Eu^{2+} ions and the lattice defects mainly oxygen vacancies. An electron excited from 4f to 5d level of europium is transferred directly to an oxygen vacancy which is subsequently released by thermal energy back to europium. This is an proposed model of an long lasting phosphorescence

(LLP) mechanism of $\text{SrAl}_2\text{O}_4:\text{Eu}$. this model is responsible for antisite defects. A mechanism for LLP ie. Long Lasting Phosphorescence whereby the antisite

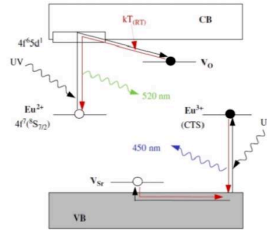


Figure 1.5: LLP mechanism of Clabau model

defect responsible for the distortion acts as a deep trap. The charging process involves trapping of an electron-hole at antisite defects of opposite charges.

1.4 Applications of LLP materials

1. **Safety Signage and Emergency Lighting:** Phosphorescent materials are commonly used in safety signage, emergency exits, and escape route markings. Their ability to glow in the dark without the need for external power sources makes them ideal for providing guidance and visibility in low-light conditions, such as during power outages or emergencies. These materials ensure that critical information remains visible even when regular lighting is unavailable.
2. **Glow-in-the-Dark Products:** Phosphorescent materials are frequently used in consumer products such as toys, stickers, clothing, and home décor items to create glow-in-the-dark effects. Children's toys, for example, often feature phosphorescent coatings or materials that glow after being exposed to light. These products provide entertainment and novelty, as well as practical visibility in the dark.
3. **Night Vision Technology:** Long-lasting phosphorescent materials have applications in night vision devices used by military personnel, law enforcement, and in civilian applications such as wildlife observation and surveillance. These materials can be integrated into instruments, goggles, and displays to provide low-light visibility without the need for active illumination sources, reducing the risk of detection.
4. **Biomedical Imaging:** In biomedical research and diagnostic imaging, phosphorescent materials are used as contrast agents to label cells, tis-

sues, or biomolecules for visualization under low-light conditions. By incorporating phosphorescent markers into biological samples, researchers can track cellular processes, study disease progression, and monitor drug delivery in real-time with high sensitivity and minimal interference from background noise.

5. **Smart Surfaces and Coatings:** Phosphorescent coatings and paints are used to create smart surfaces that absorb and store light energy during the day and emit it at night, reducing the need for artificial lighting in indoor and outdoor environments. These coatings can be applied to floors, road markings, walls, and infrastructure elements to enhance visibility, improve safety, and conserve energy.

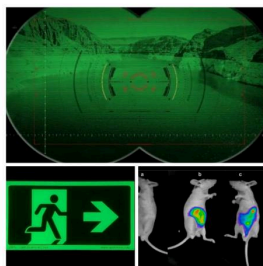


Figure 1.6: Examples of LLP

1.5 Materials of LLP

In the study of Cr^{3+} doped zinc gallate compounds, 0.5 mol% Cr^{3+} doped 1 % nominal Zn deficiency was found to be the optimum concentration to get best LLP. It was demonstrated that LLP occurred via the excitation of a specific type of Cr^{3+} ions, namely CrN_2 , having an antisite defect as first cationic neighbour. CrN_2 in the excitation, trapping and emission steps of LLP implies that CrN_2 ions are able to store visible light in $\text{ZnGa}_2\text{O}_4:\text{Cr}^{3+}$.

In $\text{MgGa}_2\text{O}_4:\text{Cr}^{3+}$, Comparison of optical studies on host lattices presented very less disorder in d-ZAO followed by d-ZGO, and a huge disorder in d-MGO. It could be directly co-related with LLP intensities observed with laser excitation wavelength corresponding to the maximum of the $^4\text{A}_2(^4\text{F}) \rightarrow ^4\text{T}_2(^4\text{F})$ absorption band of Cr^{3+} . d-ZGO with optimum defects showed maximum LLP followed by d-MGO which had large number of defects, resulting in quenching. d-ZAO no LLP intensity with less disorder displayed.

Cr^{3+} doped gallate spinels are emerging to be the widely studied long lasting phosphors, mainly because of their emission in red region. A new compound $\text{ZnGa}_2\text{O}_4:\text{Cr}^{3+}$ to be a bright LLP material with red or near infrared (NIR) light emission. A few other compounds besides aluminates and silicates, also are

Host	Dopants	Emission max.(nm)	Emission duration
SrAl ₂ O ₄	Eu ²⁺	520 (green)	30 hours
MgGa ₂ O ₄	Cr ³⁺	707 (red/NIR)	20 minutes
MgSn ₂ O ₄	Mn ²⁺	500 (green)	5 hours
ZnS	Cu ⁺	530 (green)	3 hours
BaAl ₂ O ₄	Eu ²⁺ , Dy ³⁺	500 (green)	2 hours
CaAl ₂ O ₄	Eu ²⁺ , Nd ³⁺	430 (blue)	5 hours
Sr ₂ MgSi ₂ O ₇	Eu ²⁺ , Dy ³⁺	470 (blue)	10 hours
Sr ₃ MgSi ₂ O ₈	Eu ²⁺ , Dy ³⁺	460 (blue)	10 hours
ZnGa ₂ O ₄	Cr ³⁺	695 (red/NIR)	1 hours
CaS	Eu ²⁺ , Tm ³⁺	650 (red)	1 hours

Table 1.1: List of some known persistent phosphorous

known to show LLP. These hosts include sulfides, phosphates, nitrido-silicates and borates. Most of these are used in LED research and as conversion phosphors.

1.6 Objectives

1. I prepared ZnGa₂Cr_{0.01}O₄ sample and analysed XRD, UV-Visible absorption spectroscopy, photoluminescence spectroscopy (PL excitation, PL emission) and Raman spectroscopy.
2. I analysed given data of XRD, UV-Visible absorption spectroscopy, photoluminescence spectroscopy (PL excitation, PL emission), Long Lasting Phosphorescence (LLP), Raman spectroscopy, and Anomalous XRD (A-XRD) of ZGGO sample while doping Ge⁴⁺ (0-0.40%).
3. To create antisite defects by doping ZGO to enhance LLP.

Chapter 2

Experimental techniques

2.1 Introduction

It includes sample synthesis techniques, characterizations carried out on the samples, basic working principles behind these characterizations and their instrumentation. Samples were synthesized via solid state synthesis method. Characterization carried out on the samples include XRD, UV-Visible (UV-Vis) absorption spectroscopy, Photoluminescence (PL) spectroscopy, and long lasting phosphorescence (LLP) measurements.

2.1.1 Sample preparation method

samples were synthesized by solid state method in order to obtain phase pure samples to study LLP mechanism.

Solid state synthesis

samples were synthesized using the solid state method with their respective metal oxides, ZnO (0.4539 %), Ga₂O₃ (1.0404%), CrO₃ (0.0055%). Calculated reactants were grinded in mortar along with propan-2-ol to ensure the homogeneous mixing of compounds for 1 hour. This mixture was dried in oven at 60°C for 3 hours. It was pelletized by pressing the powders under 4 tons of pressure for 5 minutes. The pellets were annealed in air at 1300°C. Pellets were cooled down to room temperature naturally and ground into fine powders.

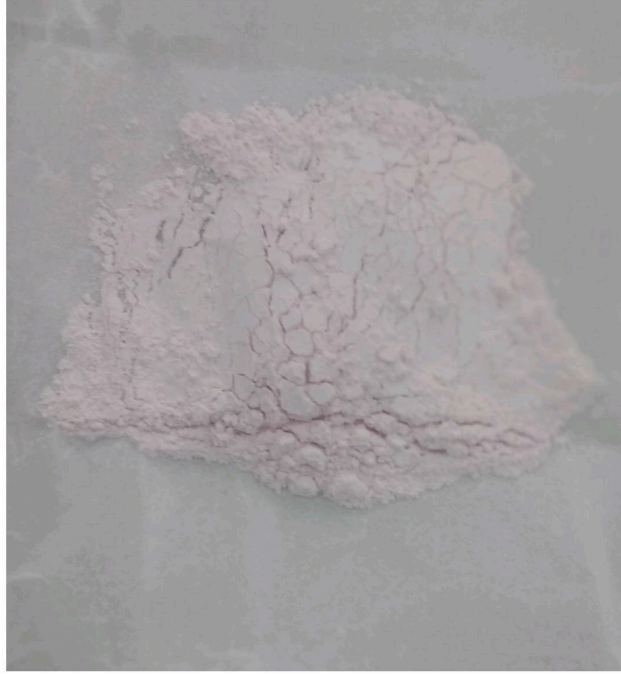


Figure 2.1: $\text{ZnGa}_2\text{Cr}_{0.01}\text{O}_4$ sample

2.1.2 X-ray diffraction

This technique is used to investigate the structure of polycrystalline powder samples and single crystals. This principle was first used in 1913 by Bragg, to obtain X-ray diffraction pattern from crystal lattice. Bragg condition states that, when X-rays are incident on a crystal lattice at a specific angle, they will undergo constructive interference if the path difference between adjacent crystal planes is equal to an integer multiple of wavelength of X-rays. It can be expressed as $2d_{hkl}\sin\theta = n\lambda$, where n is an integer. An XRD pattern is a plot of the diffracted intensity versus Bragg angle ' 2θ '.

XRD measurements were performed on powder samples with $\text{Cu-K}\alpha$ radiation source of wavelength $= 1.5418 \text{ \AA}$. XRD measurements were performed on powder samples using Rigaku X-ray diffractometer. The spectra were recorded in the 2θ range of 20° - 80° in steps of 0.02° and scan speed of 2° min^{-1} .

For these $\text{ZnGa}_2\text{Cr}_{0.01}\text{O}_4$ sample lattice constant is 8.3312 \AA . XRD indicates formation of phase pure spinel sample.



Figure 2.2: X-ray Diffraction instrument

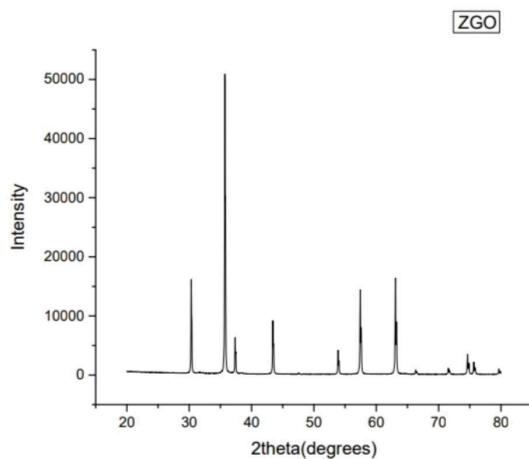


Figure 2.3: XRD graphs of $\text{ZnGa}_2\text{Cr}_{0.01}\text{O}_4$ sample

2.2 UV-Visible absorption spectroscopy

UV-Vis spectroscopy is based on the principle that molecules absorb light at specific wavelengths corresponding to transitions between electronic energy levels. When a molecule absorbs light, it promotes one or more electrons from a lower energy level (ground state) to a higher energy level (excited state). Peaks in the absorption spectrum correspond to wavelengths at which the molecule absorbs light most strongly. reflectance spectrum is converted to absorption spectrum

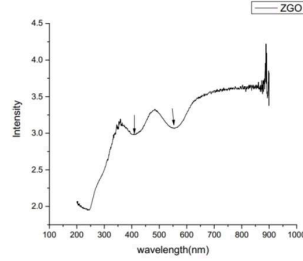


Figure 2.4: UV-Visible reflectance spectra of ZGO sample



Figure 2.5: UV-Visible instrument

using Kubelka-Munk equation which is expressed as,

$$\frac{k}{s} = \frac{(1 - R)^2}{2R} \quad (2.1)$$

where k is the molar absorption coefficient. s is the scattering coefficient and R is the absolute reflectance of the sample. Band gap of the material can be determined from the absorption spectrum using Tauc's formula,

$$\alpha h\nu = A(E_g - h\nu)^n$$

α is absorption coefficient, $h\nu$ is photon energy, E_g is band gap of the material and, A and n are constants. For direct band gap semiconductors where $n = 1/2$, a plot of $(\alpha h\nu)^2$ vs $h\nu$.

Here Fine crushed sample powder was filled into a circular sample holder and reflectance was measured in the 200 to 900 nm range, with the reflectance of barium sulphate taken as the baseline. In these UV spectrum, absorption bands shown off at around 410 nm and 560 nm. and calculated bandgap from Tauc law is 4.8 eV.

2.3 Photoluminescence spectroscopy

Photoluminescence is a phenomenon where a material absorbs photons (light energy) and then emits photons at a different wavelength. This emission typ-

ically occurs in the visible or ultraviolet spectrum. PL spectroscopy is a non-destructive technique to probe the electronic structure of the materials. It's essentially the process of light emission after absorption of photons, usually by a material.



Figure 2.6: PL instrument image

The principle behind photoluminescence spectroscopy can be,

1. **Excitation:** In photoluminescence spectroscopy, the sample is first irradiated with light of a specific wavelength or energy. This light energy is absorbed by the electrons within the material, causing them to transition to higher energy levels.
2. **Relaxation:** After absorbing the light energy, the excited electrons undergo relaxation processes. During relaxation, the electrons return to their ground state, releasing the excess energy they gained from the absorbed photons. This excess energy is emitted as photons of light, resulting in photoluminescence.
3. **Emission Detection:** The emitted light is then measured and analyzed using a spectrometer. The spectrometer detects the intensity and wavelength of the emitted light, providing information about the photoluminescent properties of the sample.

PL spectroscopy is a good technique to investigate the recombination mechanisms in luminescent materials.

2.3.1 PL excitation

The excitation process involves the absorption of photons by the material. In PL excitation spectroscopy, absorption peaks shown at 245 nm 410 nm and attributed to ${}^4A_2({}^4F) \rightarrow {}^4T_1({}^4P)$, ${}^4A_2({}^4F) \rightarrow {}^4T_1({}^4F)$, d-d transition. for these plot we are using multiple peak fitting, to find peak. Here we have used excitation wavelength as 695 nm.

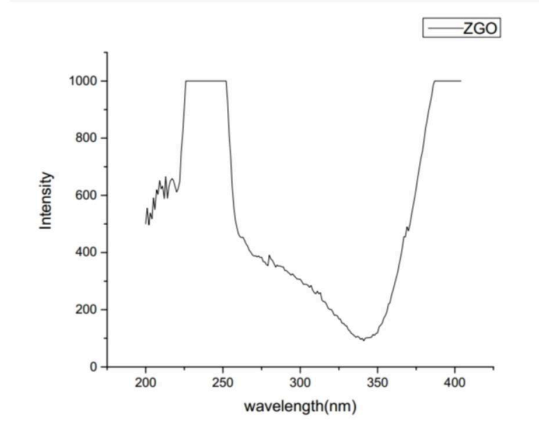


Figure 2.7: PL exc697 of ZGO sample

2.3.2 PL emission

The released photons constitute the photoluminescence emission. The wavelength of the emitted light depends on the energy difference between the excited and ground states. If the emitted light falls within the visible spectrum, it gives rise to observable luminescence.

In PL emission spectroscopy, emission resulting from ${}^2E({}^2G) \rightarrow {}^4A_2({}^4F)$ Cr^{3+}

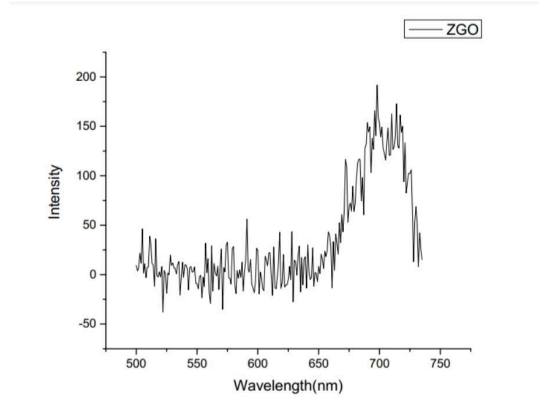


Figure 2.8: PL em200 of ZGO sample

transition. with peak emission at 697nm.

2.4 Long Lasting Phosphorescence

Long-lasting phosphorescence refers to the emission of light by a substance after it has been exposed to light or other forms of electromagnetic radiation. This persistence can range from several seconds to hours or even days, depending on the specific material.

The phenomenon occurs because some substances have electron configurations that allow them to temporarily trap the energy from incoming photons (light particles). These trapped electrons remain in excited states for an extended period before returning to their ground state and releasing the stored energy as light. Materials that exhibit long-lasting phosphorescence are often used in applications such as glow-in-the-dark toys, safety signage, and emergency lighting.

2.5 Raman Spectroscopy

Raman spectroscopy is a technique used in spectroscopy to observe vibrational, rotational, and other low-frequency modes in a system. It relies on inelastic scattering of monochromatic light, usually from a laser, typically in the visible, near infrared, or near ultraviolet range. The phenomenon is named after Indian physicist Sir C. V. Raman, who discovered it in 1928. In Raman spectroscopy, a sample is irradiated with a laser beam, and the scattered light is collected and analyzed. Most scattered photons have the same energy (frequency) as the incident photons (Rayleigh scattering), but a small fraction have different energies due to interactions with the sample's molecules. These energy differences correspond to vibrational and rotational energy levels within the molecules.

In these Raman spectroscopy, peaks shown at 715 cm^{-1} , and 609 cm^{-1} . peak of 715

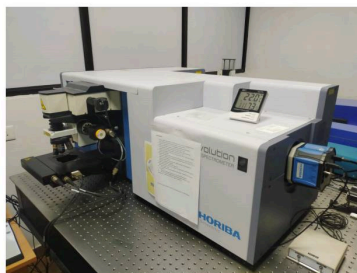


Figure 2.9: Raman spectroscopy instrument

cm^{-1} involves A_{1g} mode that is octahedral GaO_6 , and peak of 609 cm^{-1} involves T_{2g} mode in tetrahedral ZnO_4 .

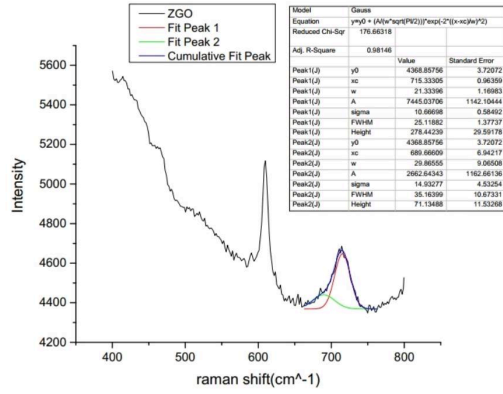


Figure 2.10: Raman spectroscopy of $\text{ZnGa}_2\text{Cr}_{0.01}\text{O}_4$ (fit.gaussianA1g)

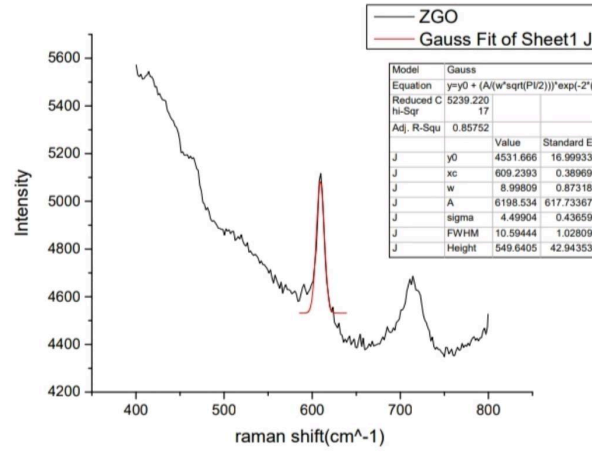


Figure 2.11: Raman spectroscopy of $\text{ZnGa}_2\text{Cr}_{0.01}\text{O}_4$ (fit.gaussianT2g)

Chapter 3

Results of ZGGO

3.1 XRD patterns

XRD patterns of representative sample (ZGGO) indicated formation of pure phase cubic spinel samples.

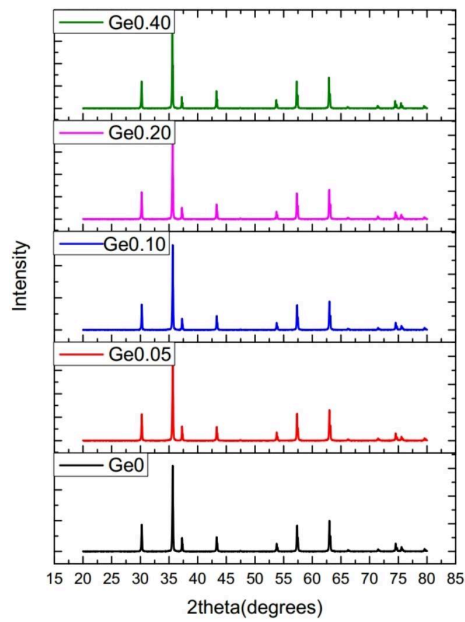


Figure 3.1: XRD graphs of ZGGO samples

In ZGGO (Zinc Gallogerminates) while doping Ge^{4+} that is (ZGGO-0%)

lattice constant is 8.3392. and (ZGGO-0.05%) lattice constant is 8.3366 Å°. and (ZGGO-0.10%) lattice constant is 8.3343 Å°. and (ZGGO-0.20%) lattice constant is 8.3473 Å°. and for (ZGGO-0.40%) lattice constant is 8.3556 Å°.

In XRD, for ZGGO sample lattice constant is starting increases and then slightly decreases and then suddenly increases because of due to the difference in ionic radii between main element and dopant ion. so, zinc is more in octahedral sites that's the reason lattice constant is increasing. so it means antisite is increasing. Ionic radii for Zn^{2+} = 0.74 Å° in tetrahedral and 0.79 Å° in octahedral. Ionic radii for Ga^{3+} = 0.62 Å° in tetrahedral and 0.76 Å° in octahedral. Ionic radii for Ge^{4+} = 0.53 Å° in tetrahedral and 0.67 Å° in octahedral.

3.2 UV-vis absorption spectroscopy

UV-visible spectra measured on reflectance mode for all ZGGO samples. calculated bandgaps from Tauc's law by fitted in linear fit for Ge^{4+} (0%) gives 4.87 eV. and doping Ge^{4+} (0.05%) in ZGGO it gives 4.71 eV. for doping Ge^{4+} (0.10%) in ZGGO it gives 4.82 eV. and Ge^{4+} (0.20%) it gives 4.83 eV. and Ge^{4+} (0.40%) it gives 4.89 eV. so, while doping germanium in Zinc gallogerminates bandgap will also be increasing.

This UV-visible spectra consists of two additional absorption bandgaps. for Ge^{4+} (0%) in ZGGO sample absorption bands shows around 410 nm and 560 nm. and for Ge^{4+} (0.05%) doped in ZGGO absorption bands at around 412 nm and 560 nm. and for Ge^{4+} (0.10%) doped in ZGGO absorption bands shows at around 411 nm and 560 nm. and for Ge^{4+} (0.20%) doped in ZGGO absorption bands shows at around 412 nm and 562 nm. and for Ge^{4+} (0.40%) doped in ZGGO absorption bands shows at around 414 nm and 562 nm. so transitions for 410 nm are from ${}^4A_2 ({}^4F) \rightarrow {}^4T_2 ({}^4F)$ and for 560 nm transitions are ${}^4A_2 ({}^4F) \rightarrow {}^4T_1 ({}^4F)$ d-d transitions.

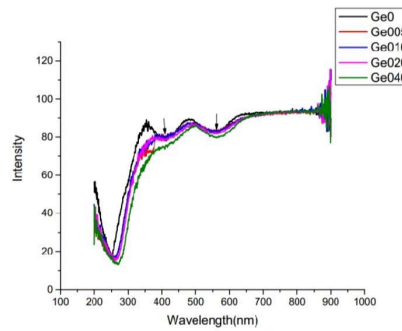


Figure 3.2: UV-visible reflectance spectra of all ZGGO samples

Thus, doping Ge^{4+} in Zinc Gallogerminates (ZGGO) can increase the slightly ab-

sorption bands because in this case, it accepts an electron from valence band, creating a hole in valence band. This hole also introduces a new energy level within the bandgap, closer to the valence band. So, the bandgap remains slightly increased, and the absorption band may shift to lower energies (longer wavelengths).

3.3 Photoluminescence Spectroscopy

3.3.1 PL excitation

In this Photoluminescence excitation spectra, three absorption bands can be fitted with Gaussian. While, Ge^{4+} (0%) doped in ZGGO, it shows absorption bands at around 560 nm and 415 nm and 290 nm. And for Ge^{4+} (0.05%) doped in ZGGO, it shows absorption bands at around 565 nm, and 416 nm and 280 nm. And Ge^{4+} (0.10%) doped in ZGGO, it shows around 570 nm, and 420 nm, and 290 nm. And for Ge^{4+} (0.20%) doped in ZGGO, it shows 573 nm, 421 nm, and 282 nm. So, the crystal field for 560 nm gives ${}^4\text{A}_2({}^4\text{F}) \rightarrow {}^4\text{T}_2({}^4\text{F})$ and 415 nm gives ${}^4\text{A}_2({}^4\text{F}) \rightarrow {}^4\text{T}_1({}^4\text{F})$ and 290 nm gives ${}^4\text{A}_2({}^4\text{F}) \rightarrow {}^4\text{T}_1({}^4\text{P})$. Bands at 410 nm and 570 nm show broadened double humps resulting from trigonal distortion and spin-orbit coupling at Ga^{3+} site. So in PL spectroscopy, crystal field increases. Crystal field increases means antisite defects are increasing so LLP decreases.

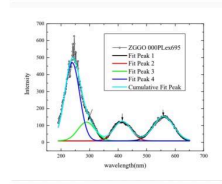


Figure 3.3: PL excitation 695 of ZGGO (0%)

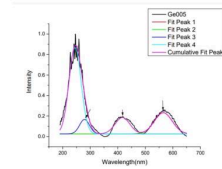


Figure 3.4: PL excitation 695 of ZGGO (0.05%)

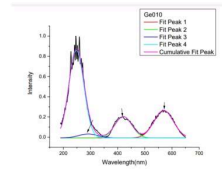


Figure 3.5: PL excitation of ZGGO (0.10%)

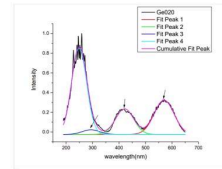


Figure 3.6: PL excitation of ZGGO (0.20%)

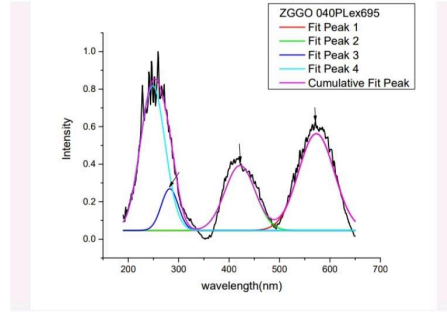


Figure 3.7: PL excitation of ZGGO (0.40%)

3.3.2 PL emission

In this spectrum, for Ge^{4+} (0%) doped in ZGGO peak emission at 695.8 nm. this shows N2 line, R line, S-PSB, AS-PSB, n7 lines. and for Ge^{4+} (0.05%) doped in ZGGO peak emission at 694.9 nm. this shows N2 lines and S-PSB. and for Ge^{4+} (0.010%) doped in ZGGO peak emission shows at 695.2 nm. this shows N2 lines and S-PSB. and for Ge^{4+} (0.20%) doped in ZGGO peak emission at 696.6 nm. this shows N2 line and S-PSB. and Ge^{4+} (0.40%) doped in ZGGO peak emission shows at 702 nm. this shows N2 line and S-PSB.

So, while Germanium doping concentration increases, for larger doping only N2 line shows. this means N2 line is unambiguously assigned to emission from Cr^{3+} ion with an antisite defect in its first cationic neighbour. mainly antisite defects responsible for N2.

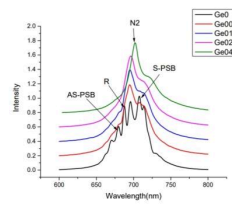


Figure 3.8: PL emission of 360 ZGGO all samples

From Tanabe sugano diagram, we can mark the crystal field transitions. while more germanium doping Ge^{4+} (0.40%) emission is decreasing.

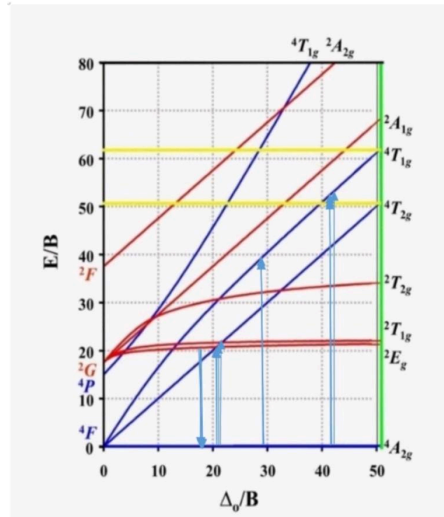


Figure 3.9: d^3 Tanabe sugano diagram for Cr^{3+} in octahedral ZGGO

3.4 Long Lasting Phosphorescence decay

LLP intensity of decay curve for ZGGO(0-0.40%) recorded after 15 minutes x-ray illumination. for Ge^{4+} (0.40%) showed the most intense LLP intensity at longer times. antisite defects responsible for N2 line are increasing which are responsible for necessitating LLP. Thus other Ge^{4+} (0-0.20%) increases in other defects (mainly Cr-Cr pairs) leads to quenching of luminescence.

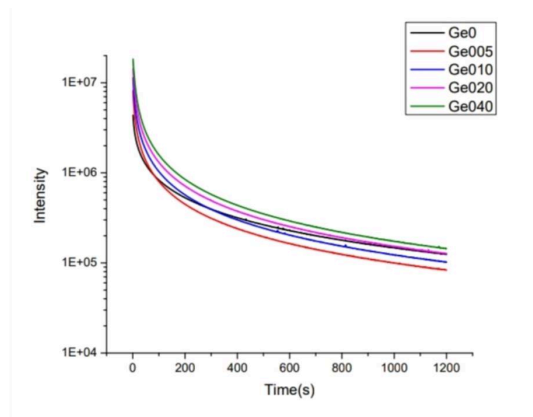


Figure 3.10: LLP decay curve of all ZGGO samples

3.4.1 LLP 360ex OnOff for ZGGO

Emission spectra obtained during X-ray illumination (X ON), 5 minutes after X-ray illumination (X OFF).for Ge^{4+} (0%) doped in ZGGO shows similar to PL spectrum showing clearly AS-PSB,N2 line,R line,S-PSB. but the LLP spectra from xray Ge^{4+} (0.40%)are largely dominated by N2 line and its PSB.Hence, it can be inferred that LLP is mainly dominated by emission from CrN_2 ions i.e., Cr^{3+} sorrounded with antisite defects.

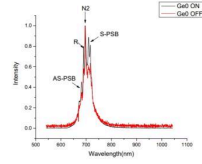


Figure 3.11: LLP 360ex OnOff for ZGGO (0%)

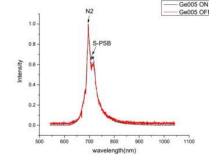


Figure 3.12: LLP 360ex OnOff for ZGGO (0.05%)

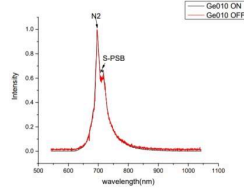


Figure 3.13: LLP 360ex OnOff for ZGGO (0.10%)

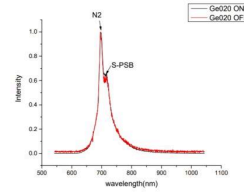


Figure 3.14: LLP 360ex OnOff for ZGGO (0.20%)

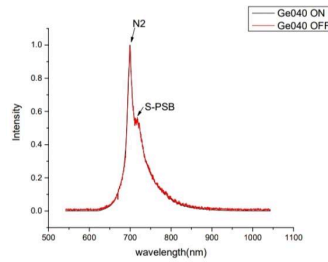


Figure 3.15: LLP 360ex OnOff for ZGGO (0.40%)

3.5 Raman spectroscopy

In raman spectroscopy,when Germanium doped, that time they shows 3 vibrational modes.the highest frequency vibrational mode assigned A1g,is characteristic of stretching vibrations of O atoms inside the octahedral unit GaO_6 .and for T2g,is the lowest energy vibrations mode are mainly due to Zn ions(ZnO_4 tetrahedral).and T1g is an intermediate frequency are related with Zn and Ga ions,with higher contribution from Ga ions.

while doping Ge^{4+} for all ZGGO samples,A1g and T2g position is increasing .it means energy is decreases it means bond is weak.for T2g amplitude is decreases it means ,no.of ZnO_4 groups with symmetric stretching vibrations are annihilated due to Ge^{4+} doping.it can be deduced that annihilated ZnO_4 group might be transferred into distorted ZnO_4 group or GaO_6 related to antisite. An additional mode at 410 cm^{-1} was observed when Ge^{4+} (0.40%)doped in ZGGO .additional mode may appear in spectra due to local lattice disorder effect likely replacement of Ga ions by heavier Ge ions.so antisite defects is occurs.

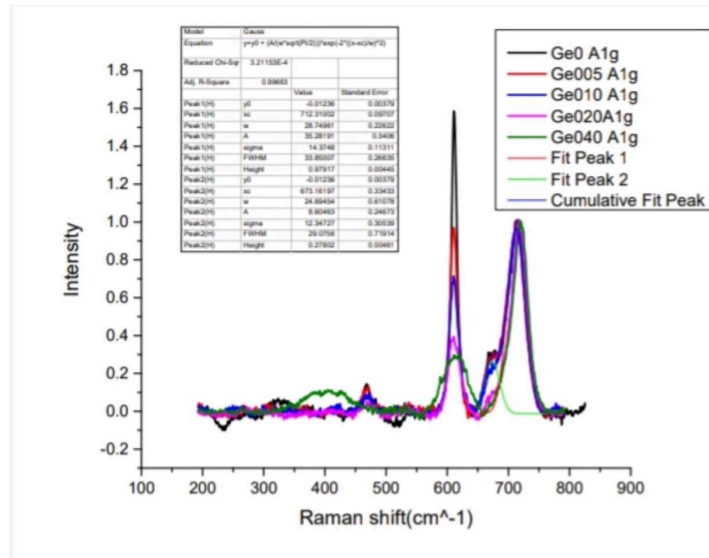


Figure 3.16: Raman spectra of all ZGGO samples (fit.gaussian) A1g mode

3.6 Anomalous XRD spectroscopy

It is an non-destructive determination technique within X-ray diffraction that makes use of the anomalous dispersion that occurs when a wavelength is selected

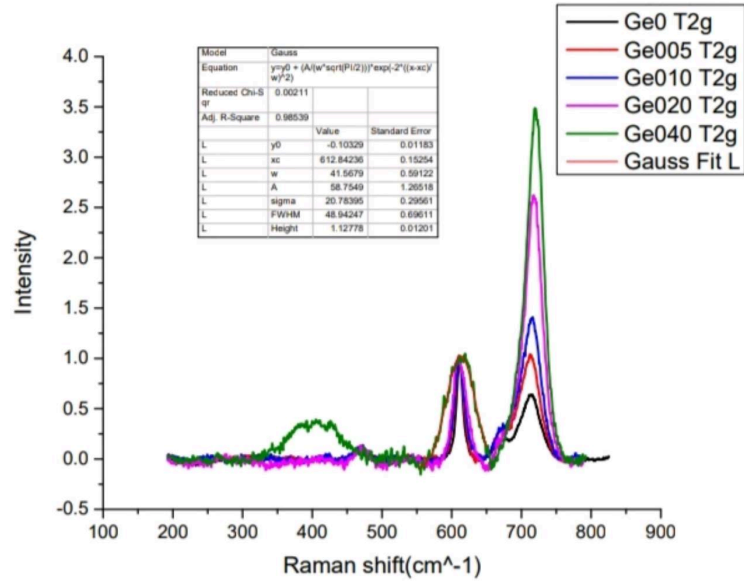


Figure 3.17: Raman spectra of all ZGGO samples (fit.gaussian T2g)

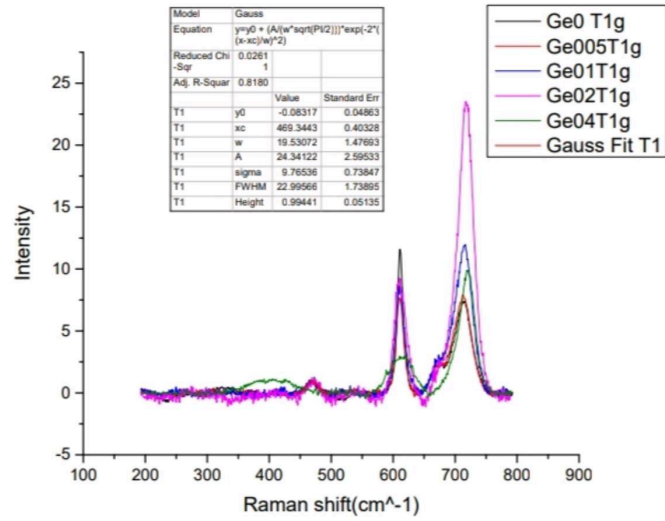


Figure 3.18: Raman spectra of all ZGGO samples (fit.gaussian T1g)

that is in the vicinity of an absorption edge of one of the constituent elements of

the sample. It is used in materials research to study nanometer sized differences in structure.

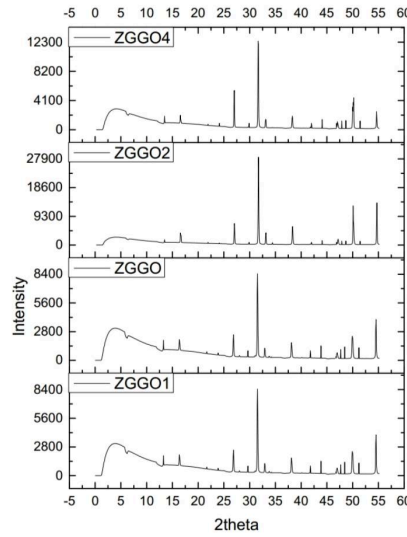


Figure 3.19: Graphs of ZGG01,ZGGO,ZGG02,ZGG04 at different energies

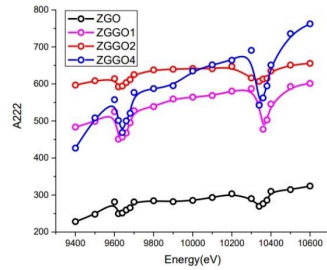


Figure 3.20: Area of 222 peak at different incident energies.

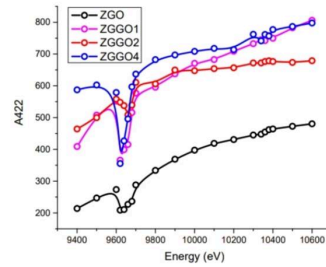


Figure 3.21: Area of 422 peak at different incident energies.

Figure(3.19):This different graphs of ZGG01,ZGGO,ZGG02,ZGG04 at different energies obtained from XRD patterns.variation of area of 222 and 422 reflection at a function obtained from XRD plots recorded at different incident energies at respective energy. Figure(3.20): This graph fitted by lorentzian fitting.and this is A222 is an octahedral sites.so,in these graph there is an slight dip it means there is an absorption of Zn K atom edge at 9600

eV. and at energy 10400 eV there also slight dip is observed it means there is an Ga K atom edge.

Figure(3.21): This graph is also fitted by Lorentzian fitting, and this is A422 is an tetrahedral sites. so, in these graph there is an slight dip is observed it means there is an Zn K atom absorption edge is at energy 9600 eV. so, in these graphs concludes that, there is an more antisite defects is an octahedral sites that is A222 because zinc atom absorption is shown off and gallium atom absorption is shown off. and A422 showing only zinc atom edge.

3.7 References

1. History of luminescence from ancient to modern times.by H. singh virk,2015.
2. Germanium oxide -doped magnesium oxide nanomaterial synthesized by green method and their characterizations study.by A.suba,P.selvarajan,J.jebaraj devadasan,2019.
3. Zinc Gallium Oxide—A Review from Synthesis to Applications.by Mu-I Chen , Anoop Kumar Singh , Jung-Lung Chiang , Ray-Hua Horng , and Dong-Sing Wu,2020.
4. Persistent luminescence: An insight, Abhilasha Jain,a,b,c,n, Ashwini Kumar,a,c, S.J. Dhoble,a,b, D.R. Peshwe,a,2016.
5. Interplay between chromium content and lattice disorder on persistent luminescence of ZnGa₂O₄:Cr³⁺ for in vivo imaging,Suchinder K. Sharma,a, Aurelie Bessière,a, Neelima Basavarajub, Kaustubh R. Priolkar, Laurent Bineta, Bruno Viana,a, Didier Gouriera,2014.
6. Nanostructured red-emitting Magnesium gallate while doping Europium phosphors,Bin-Siang Tsai, Yen-Hwei Chang, and Yu-Chung Chen,2003.
7. Optical Studies in Red/NIR Persistent Luminescent Cr-Doped Zinc Gallogermanate (ZGGO:Cr) by Maria S. Batista , Joana Rodrigues , Maria S. Relvas , Júlia Zanoni , Ana V. Girão , Ana Pimentel , Florinda M. Costa , Sónia O. Pereira , and Teresa Monteiro ,2022.
8. Red and near infrared persistent luminescence nano-probes for bioimaging and targeting applications by S. K. Singh.
9. Long-lasting luminescent ZnGa₂O₄:Cr³⁺ transparent glass-ceramics by Sébastien Chenu, Emmanuel Vérona, Cécile Genevoisa, Alain Garciaib, Guy Matzena, Mathieu Allix.
10. Long phosphorescent phosphors: From fundamentals to applications by Li, Yang, Qiu, Jianrong,2016.
11. Enhanced near infrared persistent luminescence of ZGGO while doping chromium nanoparticles by partial substitution of Germanium and tin ,Jian Yang,Hong yan,Hancheng Zhu,Meng zhang,2018.
12. Incorporation of Mg²⁺/Si⁴⁺ in ZnGa₂O₄:Cr³⁺ to Generate Remarkably Improved Near-Infrared Persistent Luminescence Shimeng Zhang, Junqing Xiahou, Xudong Sun and Qi Zhu,2022.
13. Compensation effects in GaN:Mg probed by Raman spectroscopy and photoluminescence measurements,Ronny Kirste; Marc P. Hoffmann; James Tweedie; Zachary Bryan; Gordon Callsen; Thomas Kure; Christian Nentzel; Markus R. Wagner; Ramón Collazo; Axel Hoffmann; Zlatko Sitar,2013.

14. A Pr^{3+} doping strategy for simultaneously optimizing the size and near infrared persistent luminescence of $\text{ZGGO}:\text{Cr}^{3+}$ nanoparticles for potential bio-imaging by Zheng Gong, a Yuxue Liu, *a Jian Yang, a Duanting Yan, a Hancheng Zhu, a Chunguang Liu, a Changshan Xua and Hong Zhang, 2017.
15. Preparation and characterization of a long persistent phosphor $\text{Na}_2\text{Ca}_3\text{Si}_2\text{O}_8:\text{Ce}^{3+}$ Yahong Jin, Yinrong Fu, Yihua Hu, * Li Chen, Guifang Ju, and Zhongfei Mu ,2015.
16. Storage of Visible Light for Long-Lasting Phosphorescence in Chromium-Doped Zinc Gallate Aurelie Bessiere, Suchinder K. Sharma, Neelima Basavaraju, Kaustubh R. Priolkar, Laurent Binet, Bruno Viana, Adrie J. J. Bos, Thomas Maldiney, Cyrille Richard, Daniel Scherman, and Didier Gourier, 2013.
17. Near Infrared-Emitting $\text{Cr}^{3+}/\text{Eu}^{3+}$ Co-doped Zinc Gallogermanate Persistence Luminescent Nanoparticles for Cell Imaging, Qiaoqiao Wang, Shuyun Zhang, Zhiwei Li, and Qi Zhu, 2018.
18. $\text{ZnGa}_2\text{O}_4:\text{Cr}^{3+}$: a new red long-lasting phosphor with high brightness, Aurélie Bessière, Sylvaine Jacquart, Kaustubh Priolkar, Aurélie Lecointre, Bruno Viana, and Didier Gourier, 2011.
19. N. Basavaraju, K. R. Priolkar, D. Gourier, S. K. Sharma, A. Bessière, and B. Viana. Physical Chemistry Chemical Physics, 2015.
20. T. C. Ozawa and S. J. Kang. Journal of Applied Crystallography, 2004.
21. J. Xu, J. Ueda, Y. Zhuang, B. Viana, and S. Tanabe. Applied Physics Express, 2015.
22. T. Aitasalo, D. Hreniak, J. Holsa, T. Laamanen, M. Lastusaari, J. Niitykoski, F. Pellé, and W. Strek. Journal of Luminescence, 2007.
23. T. Maldiney, A. Bessière, J. Seguin, E. Teston, S. K. Sharma, B. Viana, A. J. J. Bos, P. Dorenbos, M. Bessodes, D. Gourier, D. Scherman, and C. Richard. Nature Materials, 2014.
24. A. L. Ankudinov, B. Ravel, J. J. Rehr, and S. D. Conradson. Physical Review B: Condensed Matter and Materials Physics ,1998.
25. Katsumata T., T. Nabae, K. Sasajima, S. Komuro, and T. Morikawa. Journal of Electrochemical Society, 1997.
26. B. D. Cullity. Elements of x-ray diffraction. Addison-Wesley publishing company, 1956.
27. W. Zhang, J. Zhang, Z. Chen, T. Wang, and S. Zheng. Journal of Luminescence, 2010.